Near-adiabatic parameter changes in correlated systems: influence of the ramp protocol on the excitation energy

New Journal of Physics
The open-access journal for physics

Near-adiabatic parameter changes in correlated systems: influence of the ramp protocol on the excitation energy

Martin Eckstein[1,2] **and Marcus Kollar**[1]

[1] Theoretical Physics III, Center for Electronic Correlations and Magnetism, Institute of Physics, University of Augsburg, 86135 Augsburg, Germany
[2] Institut of Theoretical Physics, ETH Zurich, Wolfgang-Pauli-Strasse 27, 8093 Zurich, Switzerland

New Journal of Physics **12** (2010) 055012 (24pp)
Received 6 November 2009
Published 28 May 2010
Online at http://www.njp.org/
doi:10.1088/1367-2630/12/5/055012

Abstract. In this work, we study the excitation energy for slow changes of the hopping parameter in the Falicov–Kimball model with nonequilibrium dynamical mean-field theory. The excitation energy vanishes algebraically for long ramp times with an exponent that depends on whether the ramp takes place within the metallic phase, within the insulating phase or across the Mott transition line. For ramps within the metallic or the insulating phase, the exponents are in agreement with a perturbative analysis for small ramps. The perturbative expression quite generally shows that the exponent depends explicitly on the spectrum of the system in the initial state and on the smoothness of the ramp protocol. This explains the qualitatively different behaviors of gapless (e.g. metallic) and gapped (e.g. Mott insulating) systems. For gapped systems the asymptotic behavior of the excitation energy depends only on the ramp protocol and its decay becomes faster for smoother ramps. For gapless systems and sufficiently smooth ramps the asymptotics are ramp independent and depend only on the intrinsic spectrum of the system. However, the intrinsic behavior is unobservable if the ramp is not smooth enough. This is relevant for ramps to small interaction in the fermionic Hubbard model, where the intrinsic cubic fall-off of the excitation energy cannot be observed for a linear ramp due to its kinks at the beginning and the end.

Contents

1. Introduction

In equilibrium thermodynamics, adiabatic processes are defined as quasi-static processes without heat exchange with the environment. The entropy remains constant during an adiabatic process, while it always increases if the process takes place in a finite time and is therefore no longer quasi-static and reversible. These fundamental concepts are closely related to the adiabatic theorem of quantum mechanics [1]–[3] for an isolated system that evolves according to the Schrödinger equation

$$\mathrm{i}\hbar|\psi(t)\rangle = H(t)|\psi(t)\rangle, \tag{1}$$

with a time-dependent Hamiltonian $H(t)$, i.e. a system that is subject to external fields or to changes of its parameters, but not coupled to heat or particle reservoirs. The adiabatic theorem states that a system that is initially in the ground state evolves to the new ground state during an infinitesimally slow change of the Hamiltonian, whereas it cannot follow a parameter change that takes place in a finite time, resulting in a nonzero excitation energy. The paradigm for this crossover from adiabatic to nonadiabatic behavior in a quantum system is the exactly solvable Landau–Zener model [4, 5], i.e. a two-level system $H_{LZ}(t) = vt\sigma_z + \gamma\sigma_x$ that is driven through an avoided level crossing with finite speed $v > 0$ (σ_z and σ_x are Pauli matrices). When the system is in the ground state $|\phi_0(-\infty)\rangle = (1, 0)^+$ at time $t = -\infty$, the probability of finding the system in the excited state $|\phi_1(\infty)\rangle = (1, 0)^+$ at time $t \to \infty$ vanishes exponentially when the speed v is small compared to the scale $\gamma^2/\hbar$ set by the gap γ at the avoided crossing, $|\langle\psi(t \to \infty)||\phi_1(\infty)\rangle\rangle|^2 \sim \exp(-\pi\gamma^2/v\hbar)$.

The above Landau–Zener formula can be generalized to various multilevel cases [6]–[9], from which e.g. the demagnetization probability for the transverse-field Ising model was obtained [10]. However, for correlated systems in general the Landau–Zener results cannot be directly applied, because essentially all matrix elements of an interacting many-particle

Hamiltonian change in a complicated way upon variation of one of its parameters. The investigation of slow changes of external parameters in correlated systems has recently received considerable attention owing to its relevance to experiments with ultracold atomic gases in optical lattices [11], in which quantum-many-body systems can be kept under well-controlled conditions. In those systems, time-dependent control of the parameters is not only of practical importance (as discussed below) but also allows us to test fundamental theoretical predictions. For example, the Landau–Zener result was indeed experimentally confirmed in a Bose–Einstein condensate loaded into an accelerated optical lattice [12].

Various slow parameter changes in many-body systems have recently been studied [13]–[33]. For a general *ramp* the system is initially in the ground state and some parameters of the Hamiltonian are then changed to a new value within a time interval τ, either linearly or nonlinearly with time. To investigate the crossover from the extreme nonadiabatic limit $\tau = 0$ (i.e. a sudden *quench* of the Hamiltonian) to possibly adiabatic behavior in the limit $\tau \to \infty$, a measure for the degree of nonadiabaticity is needed. A popular quantity for this purpose is the excitation energy $\Delta E(\tau)$ after the ramp, i.e.

$$\Delta E(\tau) = E(\tau) - E_0(\tau), \tag{2}$$

where $E_0(\tau)$ is the ground-state energy of the Hamiltonian after the ramp. For initial states at nonzero temperature, the entropy increase provides a more natural measure of nonadiabaticity in general. However, entropy is uniquely defined only for thermal equilibrium, and thus it can only be computed after the ramp is complete and the system has thermalized. On the other hand, isolated many-body systems do not necessarily thermalize quickly after changes in the Hamiltonian [34]–[47], in particular for integrable systems, as demonstrated experimentally with ultracold gases [48]. In contrast to the entropy, the internal energy is always well defined, regardless of whether the system passes through a series of thermal or nonthermal states in the limit of a quasi-stationary process.

In the present work, we only consider systems that are initially in the ground state. If the excitation energy $\Delta E(\tau)$ vanishes in the limit of long ramp times, $\tau \to \infty$, the system is considered to behave adiabatically. It is expected that the excitation energy is still small for finite ramp times τ, just as in the Landau–Zener formula, when the ground state is protected by a gap for all parameters throughout the ramp [24]. However, the excitation energy is not exponentially small ($\Delta E(\tau) \propto \exp(\text{const}/\tau)$) in general. As we will show below, the asymptotic decrease in $\Delta E(\tau)$ for large τ can depend both on the intrinsic properties of the many-body system and on the ramp protocol. In particular for gapped systems, the ramp protocol can be used to make $\Delta E(\tau)$ arbitrarily small, but in general it often vanishes only algebraically. This behavior is known from the Landau–Zener model, where the excitation is exponentially small only when the avoided level crossing is traversed from $t = -\infty$ to $t = +\infty$, whereas the excitation probability is proportional to $1/\tau^2$ and hence is much larger if the evolution begins or ends at a finite time, e.g. at the center of the level crossing [18, 29, 49].

The situation is completely different for gapless systems, such as the exactly solvable one-dimensional transverse-field Ising model in which the gap vanishes at exactly one value of the transverse field. When the magnetic field is ramped across this critical point the excitation energy is [14]–[16]

$$\Delta E(\tau) \sim \tau^{-\eta}, \quad (\tau \to \infty) \tag{3}$$

with a rational exponent $\eta = \frac{1}{2}$. Similar results were obtained for a number of other quantum critical systems, such as the Bose–Hubbard model [21] or the random field Ising model [20].

However, the existence of a quantum critical point is not a necessary condition to obtain a nonanalytic relation $\Delta E(\tau)$ [23, 24]. Equation (3), with various values of the exponent η, holds for ramps within gapless phases of several gapless systems [24]. For a continuous bath of harmonic oscillators, which model the low-energy excitations of a large class of systems, the exponent η for a slow squeeze of the oscillator mass depends on the spatial dimension [24]: an analytic relation $\Delta E(\tau) \sim \tau^{-2}$ is found for all dimensions $d \geqslant 3$, while η is a noninteger for $d = 2$. For $d = 1$, the thermodynamic limit does not commute with the limit of large τ, i.e. the prefactor in equation (3) increases with system size [24], suggesting that adiabatic behavior is impossible for that class of one-dimensional systems.

The excitation energy during a nonadiabatic ramp, and its dependence on the ramp duration τ, is not only a fundamental property of a quantum many-body system but is also of practical interest for experiments with cold atomic gases. Various ramping procedures are used in experiments to transform one phase into another, and the available time for the process cannot be too long in order to avoid extrinsic losses. On the other hand, whether theoretical predictions are observable in experiment can depend in a subtle way on the unavoidable excitation during the preparation of the state [17], [50]–[55]. When the ramp duration is fixed to a given maximum value, it thus becomes important to find the *optimal ramp* through which a given point in parameter space can be reached through minimal excitation of the system [25]. In general, it is plausible that any additional term in the Hamiltonian should be switched on slowly, so as to build up the correlations that it favors without incurring too high an energy cost, and increasing the speed at later times.

In view of these issues, the question arises to what extent the dependence of the excitation energy on the ramp duration τ is determined by intrinsic properties of the system and to what extent it is influenced by the details of the ramp. In this paper, we give a perturbative argument that holds in the limit of small ramp amplitudes and allows us to separate an intrinsic contribution to the excitation energy and a ramp shape dependent contribution. In some cases the latter can mask the intrinsic contribution such that the behavior of the excitation energy in the limit of long ramp times τ is completely determined by the ramp shape. Furthermore, we present results for the excitation of the Falicov–Kimball model after various ramps. In this model, which can be solved exactly using nonequilibrium dynamical mean-field theory (DMFT), equation (3) is found to hold with an exponent η that is different for ramps across the metal–insulator transition, within the metallic phase, and within the insulating phase. Our numerical results for η in this model support the scenario obtained from the perturbative argument.

The paper is organized as follows. In section 2, we show results for the excitation energy in the Falicov–Kimball model in nonequilibrium DMFT. In section 3, we develop a perturbative argument for small ramp amplitudes and discuss the implications for gapped and gapless systems, such as the metallic and Mott insulating phases of the Falicov–Kimball and the fermionic Hubbard model. The conclusion given in section 4 ends the paper.

2. Ramps in the Falicov–Kimball model

2.1. Model

Below we present the results for the excitation energy $\Delta E(\tau)$ for ramps of different types in the Falicov–Kimball model [56], with the Hamiltonian

$$H_{\text{Falicov–Kimball}}(t) = \sum_{ij} V_{ij}(t)\, c_i^\dagger c_j + U(t) \sum_i n_i^f n_i^c - \mu \sum_i n_i^c - (\mu - E_f) \sum_i n_i^f . \tag{4}$$

Here $c_i^{(\dagger)}$ and $f_i^{(\dagger)}$ are annihilation (creation) operators for the itinerant and immobile electrons, respectively, and $n_i^c = c_i^\dagger c_i$ ($n_i^f = f_i^\dagger f_i$) are their local densities. Hopping between sites i and j, with amplitude $V_{ij}(t) = V(t)t_{ij}$, is possible only for the mobile c particles. Note that although the f electrons are immobile, the equilibrium state of $H_{\text{Falicov–Kimball}}$ does not correspond to one quenched f configuration but rather to a state with annealed disorder, where each f state contributes according to the free energy of the c particles.

In the context of DMFT [57], which becomes exact in infinite dimensions [58], the Falicov–Kimball model has a long history because it can be mapped onto a solvable single-site problem [59]–[62]. A Mott metal–insulator transition occurs at a critical interaction U_c for half-filling (at density $n_c = n_f = \frac{1}{2}$), as well as a transition to a charge-ordered state at sufficiently low temperatures. The physics of the Falicov–Kimball model thus partly resembles that of its parent, the fermionic Hubbard model,

$$H_{\text{Hubbard}}(t) = \sum_{ij,\sigma=\uparrow,\downarrow} V_{ij}(t) c_{i\sigma}^\dagger c_{j\sigma} + U(t) \sum_i n_{i\uparrow} n_{i\downarrow} - \mu \sum_{i,\sigma=\uparrow,\downarrow} n_{i\sigma}, \tag{5}$$

with two mobile spin species.

DMFT can be applied to nonequilibrium situations [41, 47], [63]–[70], in which case the effective single-site problem for the Falicov–Kimball model is still quadratic and can be solved using equations of motion [64]. Here we extend the exact solution of the Falicov–Kimball model for an interaction quench [41] to a numerical solution that can be applied to arbitrary time dependencies in $V(t)$ and $U(t)$ (appendix A). This allows us to study the excitation after ramps of the hopping or the interaction strength. We employ a set of hopping amplitudes for which the density of states has a semielliptic shape,

$$\rho(\epsilon) = \frac{1}{L} \sum_{\boldsymbol{k}} \delta(\epsilon - \epsilon_{\boldsymbol{k}}) = \frac{1}{2\pi} \sqrt{4 - \epsilon^2}, \tag{6}$$

where $\epsilon_{\boldsymbol{k}}$ are the eigenvalues of the hopping matrix t_{ij} and L is the number of lattice sites. Furthermore, we consider only the homogeneous phase at half-filling, for which the chemical potential is fixed at $\mu = U/2$ and the f-orbital energy at $E_f = 0$. In this case the critical interaction for the equilibrium Mott transition is $U_c = 2V$ [60].

2.2. Linear ramp protocol

We consider linear ramps in the Falicov–Kimball model (4) in DMFT for the homogeneous paramagnetic phase at half-filling. We assume that the system is in the ground state for times $t < 0$. For $0 \leqslant t \leqslant \tau$ the hopping parameter V is changed according to the ramp protocol

$$V(t) = \begin{cases} V_i, & t \leqslant 0, \\ V_i + \Delta V\, r(t/\tau), & 0 < t < \tau, \\ V_f = V_i + \Delta V, & t \geqslant \tau\,, \end{cases} \tag{7}$$

where V_i is the initial hopping amplitude, τ is the total ramp time, ΔV is the ramp amplitude and $r(x)$ is the ramp shape. The latter is a monotonously increasing function with $r(0) = 0$ and $r(1) = 1$. We set the energy scale by $V_i \equiv V \equiv 1$, so that time is measured in units of $1/V$. (From now on we set $\hbar = 1$.) The energy of the system per lattice site is given by

$$E(t) \equiv \frac{1}{L}\left[V(t) \sum_{ij} t_{ij}(t) \langle c_i^\dagger(t) c_j(t) \rangle + U(t) \sum_i \langle c_i^\dagger(t) c_j(t) f_i^\dagger(t) f_i(t) \rangle \right]. \tag{8}$$

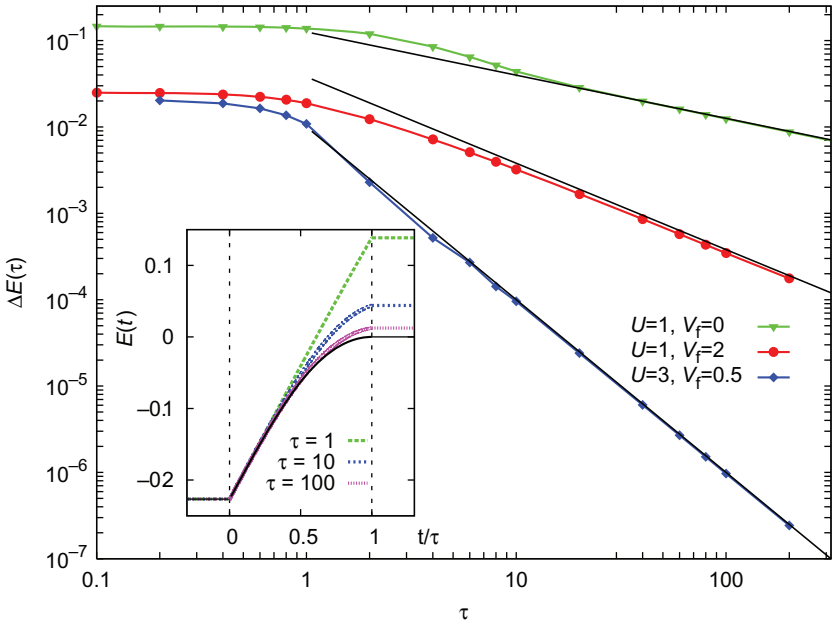

Figure 1. Excitation energy (2) after linear ramps of the hopping parameter (equation (7), $r(x) = x$) within the metallic phase ($U = 1$, $V_f = 2$), within the insulating phase ($U = 3$, $V_f = 0.5$) and across the metal-insulator transition ($U = 1$, $V_f = 0$). The energy scale is set by $V_i \equiv V = 1$. The curves become independent of τ in the quench regime $\tau \lesssim 1/V$. The solid black lines, with a slope 1/2, 1 and 2 (from the top to the bottom), correspond to the asymptotic behavior (9). Inset: Internal energy $E(t)$ (equation (8)) during ramps (7) of the hopping amplitude in the Falicov–Kimball model ($r(x) = x$, $U = 1$ and $V_f = 0$), using various ramp durations τ. For $t < 0$ and $t > \tau$, the energy is constant. The solid black line is the internal energy $E(t)$ in the ground state at $U = 1$ and hopping $V(t)$.

The excitation after a ramp is then obtained from the difference (2), where $E_0(\tau)$ is the energy (8) of the ground state of the Hamiltonian after the ramp. The DMFT solution for ramps in $V(t)$ (and also $U(t)$) is described in appendix A.

The time evolution of the energy (8) is plotted in the inset of figure 1 during a ramp (7) with linear profile $r(x) = x$. For small ramp durations ($\tau = 1$), the energy increases linearly with time. In this case, the system is essentially quenched, i.e. its state $|\psi(t)\rangle$ remains unchanged during the ramp, and the energy is thus only determined by the ramp protocol, $E(t) \approx \langle\psi(0)|H(t)|\psi(0)\rangle$. In the opposite limit $\tau \to \infty$, the energy adiabatically follows the ground-state energy $E_0(t)$ for hopping parameter $V(t)$ (solid line in the inset of figure 1), in accordance with the adiabatic theorem.

We now focus on the excitation $\Delta E(\tau)$ after the ramp, which is plotted in figure 1 for linear ramps (7) within the gapless metallic phase ($U = 1$, $V_f = 2$), within the gapped insulating phase ($U = 3$, $V_f = 0.5$) and across the metal–insulator transition ($U = 1$, $V_f = 0$), which occurs in the equilibrium system at $U = 1$ and $V = 0.5$. From figure 1 one can estimate the crossover timescale τ_{quench}, which separates the regime in which the state of the system cannot follow the parameter change ($\tau < \tau_{\text{quench}}$) from the *adiabatic regime* in which $\Delta E(\tau)$ decreases with

increasing ramp duration τ ($\tau > \tau_{\text{quench}}$). Independent of the ramp parameters, τ_{quench} turns out to be of the order of a few times the inverse bandwidth. The decrease in $\Delta E(\tau)$ for $\tau > \tau_{\text{quench}}$ can be fitted with a power law (3) for $\tau \gtrsim 10$. The exponent turns out to be a rational number, which depends only on the phase in which the system is before the ramp (metallic phase for $U < 2$, insulating phase for $U > 2$) and after the ramp (metallic phase for $U < 2V_{\text{f}}$, insulating phase for $U > 2V_{\text{f}}$). These results can be summarized as

$$\Delta E(\tau) \overset{\tau\to\infty}{\sim} \begin{cases} \tau^{-\frac{1}{2}} & \text{linear ramp across the transition,} \\ \tau^{-1} & \text{linear ramp in metallic phase,} \\ \tau^{-2} & \text{linear ramp in insulating phase.} \end{cases} \tag{9}$$

How do these exponents arise and how do they depend on the ramp shape? Further data show that the exponent $\eta = \frac{1}{2}$ for the excitation across the metal–insulator transition is independent of the ramp shape $r(x)$ (cf figure 3(b)). At present we have no simple explanation of this exponent. It would be interesting to determine how this exponent is related to the critical behavior of equilibrium correlation functions, such as the density of states at the transition [61]. On the other hand, the behavior for ramps within either the metallic or the insulating phase will be explained in the next section by a perturbative argument, which applies to small ramps of arbitrary shape in any quantum system. In particular we will see that the exponent $\eta = 1$ is a consequence of the non-Fermi-liquid behavior of the metallic phase in the Falicov–Kimball model, while the exponent $\eta = 2$ in the insulating phase is not an intrinsic property of the Falicov–Kimball model but is in fact due to the linear ramp shape.

3. Small ramps of arbitrary shape without traversing phase boundaries

Our numerical results for ramps of the hopping amplitude in the Falicov–Kimball model show that the exponent η in equation (9) does not depend on the precise values of the ramp parameters V_{i} and V_{f}, but only on the thermodynamic phase of the initial and final states. This finding suggests a study of the excitation energy perturbatively in the limit of small ramp amplitudes, but for arbitrary ramp shapes and ramp durations. In the remainder of this section we derive the excitation energy $\Delta E(\tau)$ up to second order in the ramp amplitude for an arbitrary Hamiltonian. In particular we discuss the asymptotic behavior of $\Delta E(\tau)$ in the limit $\tau \to \infty$ and how it may be influenced by the ramp shape, and we illustrate these general results with data for the specific case of the Falicov–Kimball model.

3.1. Perturbative result for the excitation energy

We consider the general Hamiltonian

$$H(t) = H_0 + \kappa(t) W, \tag{10}$$

where H_0 is the Hamiltonian before the ramp, W is the operator that is switched on and $\kappa(t)$ is the ramp function. As in equation (7), we characterize $\kappa(t)$ by the ramp amplitude $\Delta\kappa$, the ramp duration τ and the ramp shape $r(x)$, i.e. $\kappa(t) = \Delta\kappa\, r(t/\tau)$. In order to expand $\Delta E(\tau)$ for fixed ramp duration τ and ramp shape $r(x)$ in powers of $\Delta\kappa$, we decompose the quantum state $|\psi(t)\rangle$ of the system in the instantaneous eigenbasis $|\phi_n(t)\rangle$ of the Hamiltonian (10), which satisfies the condition

$$H(t)|\phi_n(t)\rangle = \epsilon_n(t)|\phi_n(t)\rangle \tag{11}$$

at any instance of time. We assume the $|\phi_n(t)\rangle$ to be nondegenerate for simplicity; in fact, only the assumption of a nondegenerate ground state is needed because transitions between excited states do not contribute to the final result below. After fixing the phase of the eigenvectors in a convenient way, we obtain the eigenstate decomposition of $|\psi(t)\rangle$ as

$$|\psi(t)\rangle = \sum_n a_n(t)\, \mathrm{e}^{-\mathrm{i}\int_0^t \mathrm{d}s\, \epsilon_n(s)}\, |\phi_n(t)\rangle, \tag{12}$$

so that the Schrödinger equation implies

$$-\frac{\mathrm{d}}{\mathrm{d}t} a_n(t) = \sum_m \mathrm{e}^{-\mathrm{i}\int_0^t \mathrm{d}s\, \epsilon_{nm}(s)}\, \langle\phi_n(t)|\frac{\mathrm{d}}{\mathrm{d}t}|\phi_m(t)\rangle, \tag{13}$$

using the notation $\epsilon_{nm}(t) = \epsilon_n(t) - \epsilon_m(t)$. The matrix element on the right-hand side of equation (13) is given by

$$\begin{aligned}\epsilon_{nm}(t)\, \langle\phi_n(t)|\frac{\mathrm{d}}{\mathrm{d}t}|\phi_m(t)\rangle &= \langle\phi_n(t)|H(t)\frac{\mathrm{d}}{\mathrm{d}t} - \frac{\mathrm{d}}{\mathrm{d}t}H(t)|\phi_m(t)\rangle \\ &= -\langle\phi_n(t)|\frac{\mathrm{d}H}{\mathrm{d}t}|\phi_m(t)\rangle \\ &= -\Delta\kappa\, \frac{r'(t/\tau)}{\tau}\, \langle\phi_n(t)|W|\phi_m(t)\rangle,\end{aligned} \tag{14}$$

where the first equality follows from equation (11) and the last from the explicit form of the Hamiltonian (equation (10)).

Because the system is assumed to be in the ground state $|\phi_0(0)\rangle$ of H_0 for $t \leqslant 0$, equation (13) must be solved with the initial condition $a_m(0) = \delta_{m0}$. Together with equation (14) this implies that $a_n(t) = \mathcal{O}(\Delta\kappa)$ for $n \neq 0$. In order to obtain the leading term in the expansion of $a_n(t)$ (for $n \neq 0$), we can thus restrict the sum in equation (13) to the single term $m = 0$,

$$a_n(t) = \Delta\kappa \int_0^t \mathrm{d}\bar{t}\, \frac{r'(\bar{t}/\tau)}{\tau}\, \frac{\langle\phi_n(\bar{t})|W|\phi_0(\bar{t})\rangle}{\epsilon_{n0}(\bar{t})}\, \mathrm{e}^{\mathrm{i}\int_0^{\bar{t}} \mathrm{d}s\, \epsilon_{n0}(s)} + \mathcal{O}(\Delta\kappa^2). \tag{15}$$

This expression was used before as a starting point for the discussion of ramps across a quantum critical point [14]. Here we study ramps that do not cross a phase boundary, and we assume that the instantaneous eigenenergies $\epsilon_{n0}(t)$ and eigenfunctions $|\phi_n(t)\rangle$, which depend on time t only through the parameter κ, can be expanded around $\kappa = 0$. Since $a_n(t)$ is already of order $\mathcal{O}(\Delta\kappa)$, $\epsilon_{n0}(t)$ and $|\phi_n(t)\rangle$ in equation (15) can be replaced by $\epsilon_{n0} \equiv \epsilon_{n0}(0)$ and $|\phi_n\rangle \equiv |\phi_n(0)\rangle$, respectively. The excitation energy, $\Delta E(\tau) = \frac{1}{L}\sum_{n\neq 0} \epsilon_{n0}(\tau)|a_n(\tau)|^2$, is then given by

$$\Delta E(\tau) = \Delta\kappa^2\, \mathcal{E}(\tau) + \mathcal{O}(\Delta\kappa^3), \tag{16}$$

$$\mathcal{E}(\tau) = \int_0^\infty \frac{\mathrm{d}\omega}{\omega}\, R(\omega) F(\omega\tau), \tag{17}$$

$$R(\omega) = \frac{1}{L}\sum_{n\neq 0} |\langle\phi_n|W|\phi_0\rangle|^2\, \delta(\omega - \epsilon_{n0}), \tag{18}$$

$$F(x) = \left|\int_0^1 \mathrm{d}s\, r'(s)\mathrm{e}^{\mathrm{i}xs}\right|^2. \tag{19}$$

Equations (16)–(19) constitute the main result of this section. The correlation function $R(\omega)$, which can be interpreted as the spectral density of possible excitations induced by the

operator W, is independent of the ramp shape $r(x)$ and the ramp duration τ. Conversely, the ramp spectrum $F(x)$ does not depend on the Hamiltonian but only on details of the ramp. For continuous ramp shapes $r(x)$ it follows that $F(x) \to 0$ for $|x| \to \pm\infty$, such that $F(\omega\tau)$ becomes increasingly peaked around $\omega = 0$ in the limit $\tau \to \infty$. In fact, making the replacement $F(\omega\tau) \propto \delta(\omega)/\tau$ is equivalent to Fermi's Golden Rule for $|a_n(t)|^2$, and the nonadiabatic excitation (17) is due to deviations of $F(\omega\tau)$ from $\delta(\omega)$. The crossover scale τ_{quench} that was discussed in section 2 is thus given by the value of τ below which $F(\omega\tau) = F(0) + \mathcal{O}(\omega^2\tau^2)$ is approximately constant over the entire bandwidth Ω of $R(\omega)$, i.e. $\tau_{\text{quench}} \approx 1/\Omega$. Note that for $\tau \lesssim \tau_{\text{quench}}$ the factor $F(\omega\tau) \approx 1$ can be taken out of the integral (17), which thus reduces to the ground-state susceptibility of the operator W with respect to the coupling parameter κ. In section 3.5 we confirm the estimate for τ_{quench} numerically for small interaction ramps in the metallic phase of the Falicov–Kimball model.

In the following, we will analyze the asymptotic behavior of equation (17) in the adiabatic limit, $\tau \to \infty$. For this we need the behavior of the ramp spectrum $F(x)$ at large values of x, which follows from equation (19) as

$$F(x) \overset{x\to\infty}{\sim} \frac{f(x)}{x^\alpha}, \quad \text{with} \quad f(x) \overset{x\to\infty}{=} \mathcal{O}(1), \tag{20}$$

where the exponent is given by $\alpha = 2n$ if the nth derivative of $r(x)$ is discontinuous (i.e. the $(n-1)$st derivative has a kink), but all lower derivatives are continuous; this behavior follows from the Riemann–Lebesgue lemma [71]. For example, in case of a linear $r(x) = x$, the first derivative $r'(x) = \Theta(x)\Theta(1-x)$ is discontinuous at $x = 0$ and $x = 1$, so that the ramp spectrum $F(x)$ decays like x^{-2} (cf equation (29*b*) below). In general, when the ramp shape has a finite number of kinks, the large-x asymptotics of the ramp spectrum (19) is given by a finite sum of oscillating terms, $F(x) \sim |\sum_k f_k \cos(\omega_k x) + \delta_k|^2/x^\alpha$. By choosing a smooth ramp one can always increase the exponent α or even make $F(x)$ decay exponentially for $x \to \infty$. However, in practice, ramp protocols often have kinks that lead to a power-law decay (20).

To estimate the magnitude of the integral (17) in the limit $\tau \to \infty$, we distinguish two cases, namely (i) the *gapless* case, in which $R(\omega)$ vanishes like a power law at $\omega = 0$, and (ii) the case of a *gapped* excitation spectrum, in which $R(\omega)$ has a finite gap Ω_{gap} above $\omega = 0$. In both cases we assume that $R(\omega)$ is zero beyond some high-frequency scale Ω, although the argument remains valid if $R(\omega)$ vanishes exponentially for $\omega > \Omega$. Since $\int_0^\infty \mathrm{d}\omega\, R(\omega) = \frac{1}{L}\left[\langle\phi_0|W^2|\phi_0\rangle - \langle\phi_0|W|\phi_0\rangle^2\right]$ we can also assume that any singularities of $R(\omega)$ are integrable.

3.2. Case (i): gapless excitation spectrum

Here we discuss the case in which the excitation spectrum $R(\omega)$ is gapless and vanishes like a power law at $\omega = 0$,

$$R(\omega) \overset{\omega\to 0}{\sim} \omega^\nu \text{ with } \nu > 0. \tag{21}$$

For example, power laws with integer exponents ν are obtained for ramps of the interaction in the metallic phase of the Hubbard model ($\nu = 3$) and the Falicov–Kimball model ($\nu = 1$) (cf equations (37) and (38) below). First we assume $\alpha > \nu$, where α is the exponent that characterizes the ramp shape (equation (20)). Writing $R(\omega) = \omega^\nu \tilde{R}(\omega)$, the integral (17) becomes, after a change of variables,

$$\mathcal{E}(\tau) = \frac{1}{\tau^\nu} \int_0^{\Omega\tau} \mathrm{d}x\, x^{\nu-1}\, \tilde{R}(x\tau^{-1}) F(x). \tag{22}$$

Using the asymptotic behavior (20) we find that the integral in this expression remains finite in the limit $\tau \to \infty$, so that in this case the leading contribution to the excitation energy is given by

$$\alpha > \nu: \quad \mathcal{E}(\tau) \overset{\tau\to\infty}{\sim} \frac{C}{\tau^{\nu}} \equiv \mathcal{E}_{\mathrm{intr}}(\tau), \tag{23}$$

with $C = \tilde{R}(0) \int_0^\infty \mathrm{d}x\, x^{\nu-1} F(x)$. It is important to note that the exponent does not depend on the ramp shape, but only on the density of possible excitations above $\omega = 0$. Because the latter is an intrinsic property of the system, we will refer to $\mathcal{E}_{\mathrm{intr}}(\tau)$ as the *intrinsic* contribution to the excitation energy in the following. In principle, a ramp between two parameter values can always be made so smooth that $\mathcal{E}_{\mathrm{intr}}(\tau)$ becomes the dominating contribution to the excitation energy (i.e. $\alpha > \nu$), as in equation (23). However, as we will see subsequently, if the ramp is not smooth enough (i.e. if $\alpha \leqslant \nu$), the intrinsic contribution will be masked by a nonuniversal contribution that is essentially determined by the ramp shape.

For the case of $\alpha \leqslant \nu$ we estimate the integral (17) as follows. For the moment we assume that the spectral density $R(\omega)$ has no singularities at finite frequencies and use the bounds

$$\omega^{\nu}\, C_1\, \Theta(\Omega_1 - \omega) \leqslant R(\omega) \leqslant \omega^{\nu}\, C_2\, \Theta(\Omega_2 - \omega), \tag{24}$$

with positive constants C_1, C_2, Ω_1, Ω_2. Together with equations (20) and (17) we obtain for the excitation energy for $\tau \to \infty$,

$$\alpha < \nu: \quad \frac{C_1'}{\tau^{\alpha}} \leqslant \mathcal{E}(\tau) \leqslant \frac{C_2'}{\tau^{\alpha}}, \tag{25}$$

$$\alpha = \nu: \quad C_1' \frac{\log(\tau\Omega)}{\tau^{\alpha}} \leqslant \mathcal{E}(\tau) \leqslant C_2' \frac{\log(\tau\Omega)}{\tau^{\alpha}}, \tag{26}$$

with positive constants C_1' and C_2'.[3] The upper bound holds because $f(x) = \mathcal{O}(1)$ in equation (20). To obtain the lower bound it is sufficient to note that although $f(x)$ can have infinitely many zeros, the moving average $\bar{f}(x) = \int_x^{x+h} \mathrm{d}x f(x)$ over any small finite interval of given length h is larger than some positive constant. This property is satisfied in particular when the ramp shape has a finite number of kinks, as discussed below equation (20). Finally, we note that equations (25) and (26) hold also if $R(\omega)$ has integrable singularities, because a small frequency interval around each of them contributes to the integral (17) in the same way as the gapped spectrum (section 3.3), namely $\propto \tau^{-\alpha}$ (equation (27)).

The result that is stated in equations (25) and (26) has a simple interpretation: kinks in the ramp shape increase the probability of excitations to high-energy states, as expressed by the slowly decaying tail of the ramp spectrum $F(x)$. When the ramp is not smooth enough, the integral (17) is therefore dominated by the high-frequency part of $R(\omega)$, leading to a nonuniversal, ramp-shape-dependent excitation energy. For the often-considered linear ramp ($\alpha = 2$), any intrinsic contribution $\mathcal{E}_{\mathrm{intr}}(\tau)$ with $\nu \geqslant 2$ will therefore be unobservable in $\mathcal{E}(\tau)$. This is precisely what happens for weak-coupling interaction ramps in the Hubbard model, as discussed below in section 3.5.

[3] Equations (25) and (26) may be expressed as $\mathcal{E}(\tau) = \Theta(1/\tau^{\alpha})$ and $\mathcal{E}(\tau) = \Theta(\log(\tau\Omega)/\tau^{\alpha})$, respectively, where $f(x) = \Theta(g(x))$ is the Bachmann–Landau *Big Theta* notation for the fact that there exist constants K_1 and K_2 such that $K_1|g(x)| \leqslant |f(x)| \leqslant K_2|g(x)|$ for sufficiently large x (not to be confused with the Heaviside step function $\Theta(x)$). This is a stronger statement than $f(x) = \mathcal{O}(g(x))$, which implies only the upper bound, but a weaker statement than $f(x) \sim g(x)$, which means that $\lim_{x\to\infty}|f(x)/g(x) - 1| = 0$.

3.3. Case (ii): gapped excitation spectrum

We now turn to the case of an excitation density that has a gap Ω_{gap} at $\omega = 0$. The integral (17) then starts at the finite lower bound Ω_{gap}, such that $F(x)$ can be replaced by its asymptotic behavior (20) in the entire integration range. As a consequence we have

$$\mathcal{E}(\tau) \overset{\tau\to\infty}{\sim} \frac{1}{\tau^{\alpha}} \int_{\Omega_{\mathrm{gap}}}^{\Omega} \mathrm{d}x \; \frac{R(x)\, f(x\tau)}{x^{\alpha+1}}. \tag{27}$$

The integral gives a finite constant in the limit $\tau \to \infty$ provided that $R(\omega)$ is not singular. Otherwise the integral may give a τ-dependent but bounded contribution, as shown in the next subsection for ramps in the insulating phase of the Falicov–Kimball model. The gapped case (equation (27)) is thus similar to the gapless case with $\alpha < \nu$ (equation (25)). In both cases the excitation energy is dominated by the high-frequency behavior of $F(x)$ and is therefore completely determined by the ramp shape, while the intrinsic contribution (23) is unobservable.

Our analysis so far can be summarized as follows. The excitation energy after a ramp may be either dominated by the intrinsic contribution (23) or set by ramp-shape-dependent terms (equations (25)–(27)), depending on the large-frequency asymptotics (20) of the ramp spectrum and the small-frequency behavior (21) of the excitation density. Our results for the gapless phase are consistent with recent investigations that use adiabatic perturbation theory [29, 72] to study power-law ramps in quantum critical systems [30, 33], including gapless noncritical systems as a limiting case. Furthermore, adiabatic perturbation theory for linear ramps in gapped systems proves that the excitation energy is determined by the square of the derivative of the quench parameter with time [29]. Because this derivative also determines the large-x asymptotics (20) of the ramp spectrum $F(x)$, the latter result is consistent with our equation (27). In the remainder of this paper we will illustrate the general results of the preceding subsections for ramps in the insulating and the metallic phase of the Falicov–Kimball model and the Hubbard model.

3.4. Insulating phase

In the previous subsection, we have shown that the excitation energy after a ramp within a gapped phase behaves in a nonuniversal way because the intrinsic contribution (23) vanishes. A significant dependence of the nonadiabatic excitation energy on the ramp shape is therefore expected also for ramps with finite amplitude. In the following we will demonstrate this fact for ramps within the insulating phase of the Falicov–Kimball model, where it turns out that the asymptotic behavior for $\tau \to \infty$ is indeed correctly described by the analytic expression (27) that was obtained for small ramps.

For this purpose we focus on three particular ramp shapes,

$$r_1(x) = x, \tag{28a}$$

$$r_2(x) = \frac{1 - \cos(\pi x)}{2}, \tag{28b}$$

$$r_3(x) = \frac{\pi x - \cos(\pi x)\sin(\pi x)}{\pi}. \tag{28c}$$

Here $r_n(x)$ is chosen in such a way that its nth derivative is discontinuous at $x = 0$ and $x = 1$ (figure 2(a)), i.e. $r_n'(x) \propto \sin^n(\pi x)$ for $0 < x < 1$. The corresponding ramp spectra

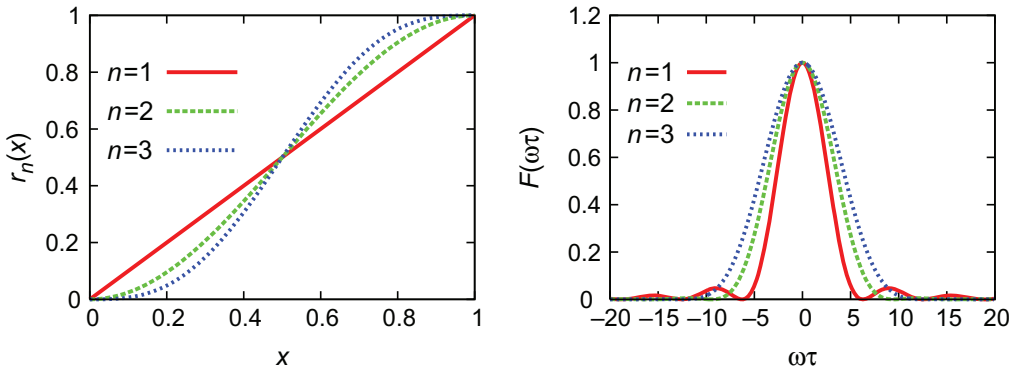

Figure 2. Ramp shapes given by equations (28*a*)–(28*c*) (left panel) and corresponding ramp spectra (equations (29*a*)–(29*c*)) (right panel). The Fresnel oscillations in $F_n(\omega)$ are due to the discontinuity in the derivatives of $r_n(x)$ at $x = 0$ and $x = 1$.

(equation (19)) are

$$F_1(\omega) = 2\,\frac{1-\cos(\omega)}{\omega^2}, \tag{29a}$$

$$F_2(\omega) = \frac{\pi^4}{2}\,\frac{1+\cos(\omega)^2}{(\pi^2-\omega^2)^2}, \tag{29b}$$

$$F_3(\omega) = 32\pi^4\,\frac{1-\cos(\omega)}{\omega^2(4\pi^2-\omega^2)^2}. \tag{29c}$$

These functions vanish like $F_n(x) \sim x^{-2n}$ for $x \to \infty$ (figure 2(b)). We now perform ramps of the hopping amplitude $V(t) = V_i + (V_f - V_i)\, r_n(t/\tau)$ in the Falicov–Kimball model, with $V_i = V = 1$ as the energy scale. We consider only the paramagnetic insulating phase at half-filling, i.e. $U > 2 = 2V_i$ and $U > 2V_f$.

The excitation energy after such ramps is plotted as a function of the ramp duration τ in figure 3(a). The curves can be fitted with power laws (3) for large τ, with an exponent $\eta = 2$ for the linear ramp (28*a*) and $\eta = 4$ for the ramp (28*b*), respectively. For the ramp (28*c*) the results are consistent with an exponent $\eta = 6$, but the excitation energy is too small for a power-law fit in the accessible range. Hence, the large-τ behavior of the nonadiabatic excitation in the case of ramps with finite amplitude turns out to be the same as in the limit of small ramps, i.e. a power law with an exponent that is determined by the singularities of the derivatives of the ramp shape (cf equation (27)) rather than by intrinsic properties of the system. As mentioned in section 2, such a dependence of the excitation energy on the ramp shape is not observed in ramps across the metal–insulator transition; instead the same exponent $\eta = \frac{1}{2}$ is obtained for the three ramps (28*a*), (28*b*) and (28*c*) (figure 3(b)).

To check equation (17) explicitly for arbitrary ramps we would have to compute the density of excitations $R(\omega)$, for which no general solution is available. Nevertheless one can derive an expression in the atomic limit and compare the resulting excitation energy to ramps deep in the insulating phase. For ramps of the hopping $V(t)$, the operator W in equation (18) is given by the kinetic energy operator. In the case of half-filling for both mobile and immobile particles there is exactly one particle per site in the ground state for $V = 0$. Therefore each hopping process

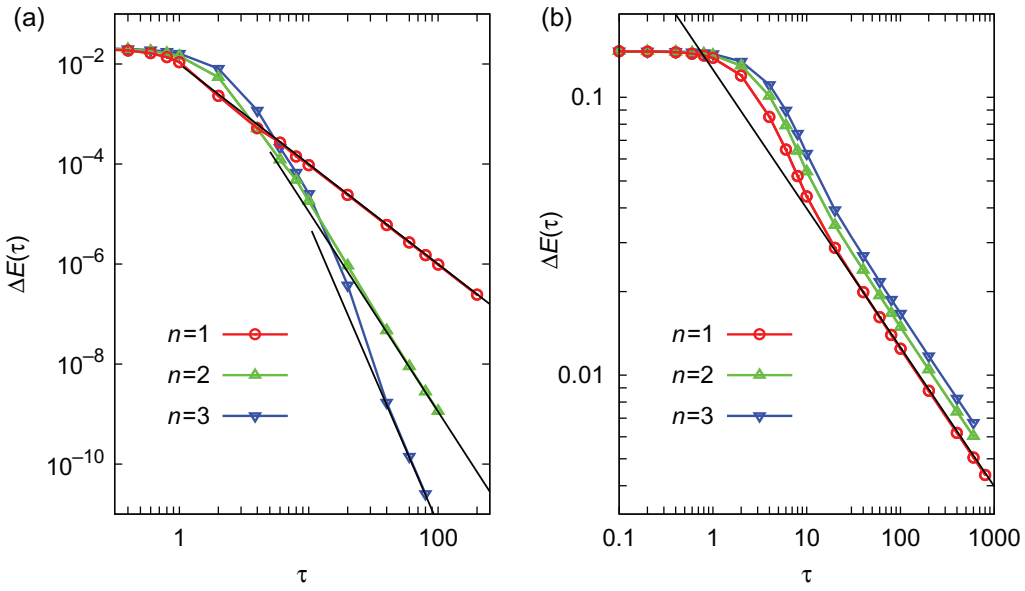

Figure 3. The same as figure 1, for ramps $r(x) = r_n(x)$ (equations (28*a*)–(28*c*)). (a) Ramps within the insulating phase, $U = 3$, $V_f = 0.5$. The black linear lines correspond to power-law behavior (3) with $\eta = 2$ ($n = 1$) and $\eta = 4$ ($n = 2$), and $\eta = 6$ ($n = 3$). (b) Ramps across the metal–insulator transition, $U = 1$, $V_f = 0$. The black linear line corresponds to power-law behavior (3) with $\eta = \frac{1}{2}$.

creates exactly one doubly occupied site, and the function $R(\omega)$ consists of a single delta peak at $\omega = U$. When $R(\omega) \propto \delta(\omega - U)$ is inserted into equation (17), one obtains

$$\Delta E(\tau) \propto F(U\tau), \tag{30}$$

i.e. the Fresnel oscillations in ramp spectra such as equations (29*a*)–(29*c*) become visible in the dependence of the excitation energy on τ. This result should only be slightly modified for ramps deep in the insulating phase ($U \gg V$), assuming that the delta-peak is then only slightly broadened and shifted in position. In fact, as shown in figure 4 the tail oscillations of $F_1(x)$ (equation (29*a*), figure 2) are also apparent in the excitation energy for ramps between states with $U \gg V$. In the limit $\tau \to \infty$ these oscillations are washed out because $R(\omega)$ has a finite bandwidth $\Delta\Omega$ for $V > 0$, such that the integral (17) averages over many oscillations for $\tau \gg 1/\Delta\Omega$.

3.5. Metallic phase

As an application of equation (17) to ramps in a gapless phase, we consider the turn-on of the interaction in the Falicov–Kimball model and the Hubbard model. For the following discussion it is convenient to write the Hamiltonian in momentum space:

$$H = \sum_{k\sigma} (\epsilon_{k\sigma} - \mu_\sigma) c^\dagger_{k\sigma} c_{k\sigma} + U(t) D, \tag{31}$$

$$D = \sum_i n_{i\downarrow} n_{i\uparrow} = \sum_{k,k',q} c^\dagger_{k+q\downarrow} c_{k\downarrow} c^\dagger_{k'-q\uparrow} c_{k'\uparrow}. \tag{32}$$

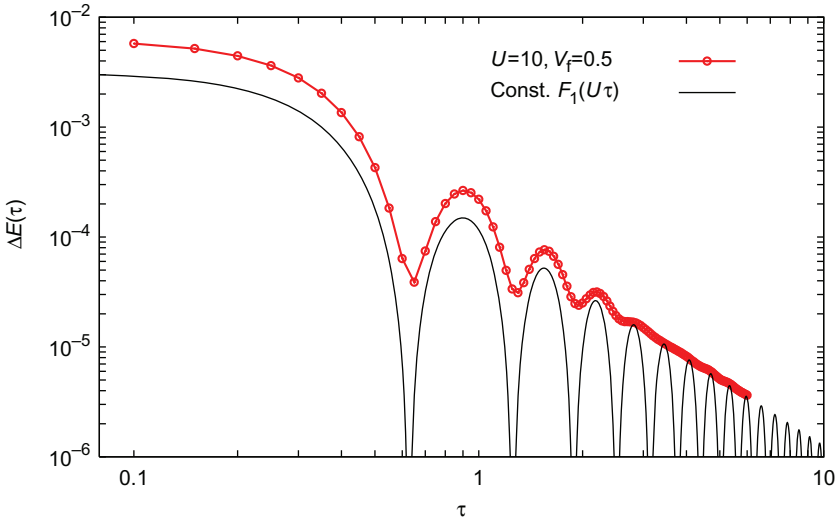

Figure 4. Excitation energy 2 after the linear ramp (28*a*) of the hopping amplitude within the insulating phase ($U = 10$, $V_i = 1$, $V_f = 0.5$), compared to equation (30) for small ramp amplitudes (F_1 given by equation (29*a*)).

Furthermore, we change the notation with respect to equation (4) to allow for a unified description of the Hubbard model, where both spin species are mobile ($\epsilon_{k\uparrow} = \epsilon_{k\downarrow}$, $\mu_\uparrow = \mu_\downarrow$) and the Falicov–Kimball model, where we take spin $\uparrow$ to be immobile ($\epsilon_{k\uparrow} = 0$, $\mu_\uparrow = \mu - E_f$, $\mu_\downarrow = \mu$). We consider ramps at half-filling ($\mu_\sigma = U/2$) in which the interaction is changed from zero to a finite value, $U(t) = \Delta U r(t/\tau)$.

For a ramp of the interaction strength in the Hubbard model and the Falicov–Kimball model, the operator W in equation (10) is given by the double occupation (32). As shown in appendix B, the excitation density $R(\omega)$ at $U = 0$ can be expressed in terms of the second-order contribution to the self-energy

$$R(\omega) = -\frac{1}{\pi} \sum_{-\omega \leqslant \epsilon_{q\downarrow} \leqslant 0} \mathrm{Im}\, \Sigma^{(2)}_{q\downarrow}(\omega + \epsilon_{q\downarrow} + \mathrm{i}0). \tag{33}$$

For comparison to our DMFT results we evaluate equation (33) in the limit of infinite dimensions [58] where the self-energy is independent of momentum $\boldsymbol{q}$ [73] and the $\boldsymbol{q}$-summation can be replaced by an integral over the density of states $\rho_\downarrow(\epsilon)$,

$$R(\omega) = -\frac{1}{\pi} \int_{-\omega}^{0} \mathrm{d}\epsilon\, \rho_\downarrow(\epsilon)\, \mathrm{Im}\, \Sigma^{(2)}_\downarrow(\epsilon + \omega + \mathrm{i}0). \tag{34}$$

For the Hubbard model, the second-order self-energy is given by [73]

$$-\frac{1}{\pi} \mathrm{Im}\, \Sigma^{(2)}_{\mathrm{Hub}}(\omega) = \int_0^\omega \mathrm{d}\mu\, \rho(\mu - \omega) \int_0^\mu \mathrm{d}\nu\, \rho(\nu)\rho(\mu - \nu) \overset{\omega \to 0}{\sim} \tfrac{1}{2}\, \rho(0)^3\, \omega^2. \tag{35}$$

In accordance with Fermi liquid theory, the imaginary part of the self-energy vanishes $\propto \omega^2$, thus leading to well-defined quasi-particle excitations in the metallic phase of the Hubbard model. On the other hand, the imaginary part of the mobile electron self-energy in the Falicov–Kimball model remains finite at $\omega = 0$ due to the scattering of fixed impurities. Its value can be obtained

easily from the exact solution of the Falicov–Kimball model in DMFT [62],

$$-\frac{1}{\pi}\mathrm{Im}\,\Sigma^{(2)}_{\mathrm{FKM}}(\omega) = (1-n_{\mathrm{f}})n_{\mathrm{f}}\rho(\omega) \overset{\omega\to 0}{\sim} (1-n_{\mathrm{f}})n_{\mathrm{f}}\rho(0). \tag{36}$$

Here n_{f} is the average density of localized particles, such that $n_{\mathrm{f}} = 0.5$ in the case of half-filling. Equations (35) and (36) can then be inserted in equation (34), which in turn determined the intrinsic component (23) of the excitation energy,

$$\text{Hubbard}: R(\omega) \overset{\omega\to 0}{\sim} \tfrac{1}{6}\rho(0)^4\omega^3 \Rightarrow \mathcal{E}_{\mathrm{intr}}(\tau) \propto \tau^{-3}, \tag{37}$$

$$\text{Falicov–Kimball}: R(\omega) \overset{\omega\to 0}{\sim} (1-n_f)n_f\rho(0)^2\omega \Rightarrow \mathcal{E}_{\mathrm{intr}}(\tau) \propto \tau^{-1}. \tag{38}$$

Although we have derived these equations for the limit of infinite dimensions, they remain valid under more general assumptions. In fact, from equation (34) a power law $R(\omega) \sim \omega^{\nu}$ is obtained if (i) the density of states is finite at $\omega = 0$ and (ii) one has $\mathrm{Im}\,\Sigma_{\boldsymbol{q}}(\omega) \sim \omega^{\nu-1}$ for $\omega \to 0$. The weaker excitation energy in the Hubbard model thus stems from the fact that its metallic state is a Fermi liquid [$\mathrm{Im}\,\Sigma_{\boldsymbol{q}}(\omega) \sim \omega^2$], whereas this is not the case for the Falicov–Kimball model due to impurity scattering [$\mathrm{Im}\,\Sigma_{\boldsymbol{q}}(\omega) \sim$ const]. Physically speaking, the creation of electron–hole pairs by the interaction operator is strongly suppressed at low energies in the Hubbard model, so that few low-lying excitations are present in the intrinsic contribution to the excitation energy.

As discussed above, the intrinsic contribution can be masked completely by a ramp-shape-dependent contribution if the ramp is not smooth enough, i.e. when the exponent in equation (20) satisfies $\alpha \leqslant 1$ or $\alpha \leqslant 3$ in the case of the Falicov–Kimball and the Hubbard model, respectively. However, the discussion below equation (20) shows that $F(x)$ decays at least $\propto x^{-2}$ if the ramp is continuous, i.e. if it does not contain any abrupt finite changes. Hence we conclude that the intrinsic component (38) is always dominant for ramps that turn on a small interaction in the Falicov–Kimball model. This is consistent with our numerical results for ramps in the metallic phase of the Falicov–Kimball model, which are not shown here, namely that the $1/\tau$ behavior for the metallic phase in (9) does not only hold for linear ramps (figure 1), but for all three ramps (28*a*)–(28*c*).

The situation is very different for ramps in the Hubbard model. Because the intrinsic contribution (37) vanishes $\propto \tau^{-3}$ for $\tau \to \infty$ it is negligible with respect to the high-frequency contribution (25) for linear ramps, where the ramp spectrum decays as x^{-2} (equation (29*a*)). This is consistent with the results of Möckel and Kehrein [32], who computed the excitation energy after a linear ramp of the interaction in the Hubbard model using the Keldysh perturbation theory and found $\Delta E(\tau) \sim \tau^{-2}$ for $\tau \to \infty$.

The exact expression for $R(\omega)$ at all frequencies in the Falicov–Kimball model at $U = 0$ (equations (34) and (36)) allows us to evaluate $\mathcal{E}(\tau)$ for arbitrary interaction ramps $U(t) = \Delta U r(t\tau)$ at finite ramp durations, and compare to the DMFT result for $\Delta E(\tau)$. In figure 5 this comparison is done for a smooth *Gaussian ramp* (inset (a) in figure 5), which we define by

$$r'(x) = c_1 \exp\left[-c_2(x-1/2)^2\right], \tag{39}$$

$$F(x) = \frac{\pi c_1^2}{c_2}\exp\left(-\frac{x^2}{4c_2}\right) \quad \text{for} \quad c_2 \gg 1, \tag{40}$$

where c_1 is a normalization constant to satisfy the condition $\int_0^1 \mathrm{d}x\, r'(x) = r(1) - r(0) = 1$, and c_2 is chosen such that $r'(x)$ is sufficiently small at the boundary $x = 0$ and $x = 1$, i.e. the

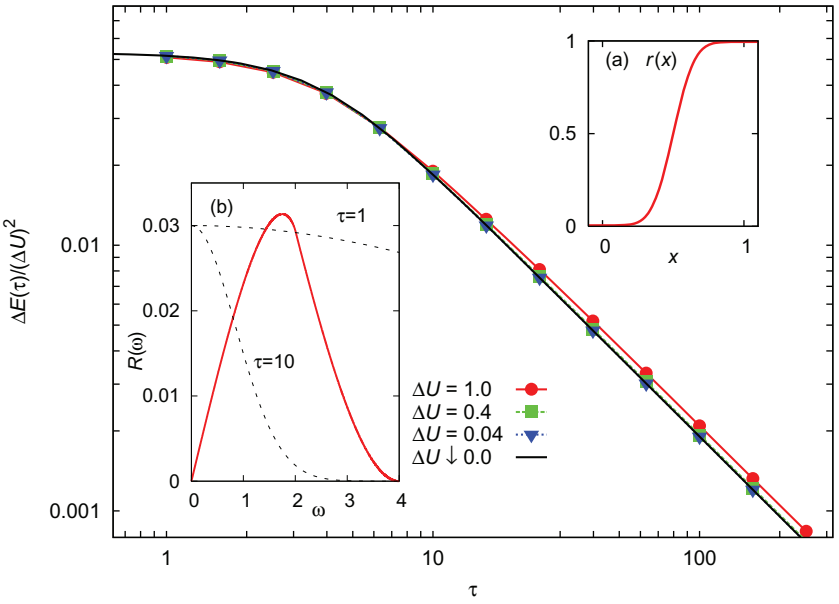

Figure 5. Excitation $\Delta E(\tau)$ in the metallic phase of the Falicov–Kimball model, after Gaussian ramps (equation (39), $c_2 = 36$, see inset (a)) from interaction $U = 0$ to ΔU. The curve $\Delta U = 0$ is obtained from equation (17), where $R(\omega)$ is obtained from equations (34) and (36), and $F(\omega)$ is given by equation (39). The excitation spectrum $R(\omega)$ (solid line) is plotted in inset (b), together with $0.03\, F(\omega\tau)$ (dashed lines) to illustrate the effect of τ (see text).

expression for $F(x)$ holds up to terms that are exponentially small in c_2. For $U \lesssim 1$, numerical results for the excitation energy (scaled with the ramp amplitude ΔU^2) agree very well with the analytical expression (17), evaluated using equations (34), (36) and (40). This corroborates the validity argument of section 3 and shows that it provides correct estimates for the nonadiabatic excitation energy after ramps that are not too large in amplitude.

Inset (b) of figure 5 illustrates the origin of the crossover from small to large ramp times τ. For fast ramps, e.g. $\tau = 1$, the ramp spectrum $F(\omega\tau)$ averages over the entire bandwidth Ω of the excitation spectrum $R(\omega)$. As a consequence, the excitation energy becomes independent for ramp times smaller than the quench timescale $\tau \lesssim 1/\Omega = \tau_{\text{quench}}$. Indeed we see in the numerical data that the weak-coupling quench timescale fits with the estimate $1/\Omega \approx 1/4$. For larger quench times, e.g. $\tau \gtrsim 10$ in inset (b) of figure 5, the ramp spectrum $F(\omega\tau)$ probes only the linear small-ω behavior of $R(\omega)$, leading to the universal power-law behavior $\Delta E(\tau) \sim 1/\tau$ for $\tau \gtrsim 10$.

4. Conclusion

We presented a general perturbative analysis of the excitation energy due to slow ramps of a parameter in a quantum system without crossing of phase boundaries, motivated by our numerical results for the Falicov–Kimball model obtained with nonequilibrium DMFT. We demonstrated that the excitation energy vanishes algebraically for large ramp duration τ (equation (3)) under rather general circumstances. The exponent η can depend, on the one hand,

on the spectrum of the correlation function of the operator that is switched on and, on the other hand, on the differentiability of the ramp function. Which of these influences dominates in η depends on the low-energy behavior of the excitation spectrum compared to the spectrum of the ramp protocol. In practice, any experimental ramp protocol can always be considered as differentiable on a short enough timescale. Our conditions on the degree of differentiability have to be interpreted in the sense that a ramp protocol must be considered as not differentiable if the slope or any higher derivative changes on a timescale shorter than the inverse bandwidth of the system.

For ramps in gapped systems the asymptotic behavior of the excitation energy depends only on the ramp protocol and can be made as small as desired by the use of increasingly smooth ramp shapes. By contrast, for ramps in gapless systems the low-energy excitation spectrum has no effect on η if the ramp is not smooth enough. Only if the ramp is sufficiently smooth does η become ramp independent and reflect the low-energy excitation spectrum of the system. For the fermionic Hubbard model this implies that a linear ramp from $U = 0$ to a small value of U leads to an unnecessarily large excitation energy with $\eta = 2$, which can be reduced to the intrinsic exponent $\eta = 3$ if the ramp shape has at least two continuous derivatives.

Our results also indicate that in the Falicov–Kimball model the exact expression for the excitation energy in the limit of small ramps provides a good estimate up to quite large ramp amplitudes. This suggests the use of the perturbative expression, which is valid for arbitrary systems, as a guide for finding ramp protocols that connect fixed parameters of the Hamiltonian and minimize the excitation energy for a given ramp time, thereby improving the preparation of states in experiments with ultracold atomic gases.

Acknowledgments

Useful discussions with Stefan Kehrein are gratefully acknowledged. ME acknowledges support from Studienstiftung des deutschen Volkes. This work was supported in part by SFB 484 of the Deutsche Forschungsgemeinschaft.

Appendix A. Solution of the Falicov–Kimball model in nonequilibrium using DMFT

In this appendix, we describe in some detail how the Falicov–Kimball model (4) with arbitrary time-dependent hopping amplitude $V(t)$ or time-dependent interaction $U(t)$ is solved using nonequilibrium DMFT[4]. In DMFT, local correlation functions of the lattice model are obtained from an effective impurity model in which a single site is coupled to a self-consistently determined environment [57]. The mapping of the lattice model onto the single-site model, which becomes exact in the limit of infinite dimensions [58], can be formulated either in imaginary time, which yields a theory for thermal equilibrium, or in real time (using the Keldysh technique), which yields a theory that can be applied to various nonequilibrium situations [63]. For the Falicov–Kimball model the action of the single-site model can be reduced to a quadratic one [59], such that nonequilibrium correlation functions can be determined from a closed set of equations of motion [41], [64]–[69].

Because we are interested in the transient time evolution of a system that is in thermal equilibrium for times $t \leqslant 0$ (i.e. its initial state is given by the density matrix $\rho \propto \exp[-\beta H(0)]$),

[4] In the appendices, τ denotes imaginary time, not to be confused with the ramp duration τ in the main text.

we use contour-ordered Green functions with time arguments on the contour $\mathcal{C}$ that runs from $t = 0$ to $t_{\max}$ (the maximum simulated time) on the real axis, back to $t = 0$, and finally to $t = -\mathrm{i}\beta$ along the imaginary axis [74]. The local Green function is then given by

$$G(t, t') = -\mathrm{i}\frac{1}{Z}\mathrm{Tr}\left[\mathrm{e}^{-\beta H(0)}\mathrm{T}_{\mathcal{C}}\,\hat{c}(t)\hat{c}^{\dagger}(t')\right], \tag{A.1}$$

where $\mathrm{T}_{\mathcal{C}}$ is the contour ordering operator, and $\hat{c}^{(\dagger)}(t)$ are annihilation (creation) operators of the mobile particles in the Heisenberg picture with respect to the time-dependent Hamiltonian. Up to a factor 'i' the imaginary-time Green function of the interacting equilibrium state is recovered from equation (A.1) when both time arguments are on the imaginary-time portion of the contour. On the other hand, when both time arguments are on the real branch we obtain the real-time Green functions $G^{<}(t, t') = \mathrm{i}\mathrm{Tr}[\mathrm{e}^{-\beta H(0)}\hat{c}^{\dagger}(t')\hat{c}(t)]$ and $G^{>}(t, t') = -\mathrm{i}\mathrm{Tr}[\mathrm{e}^{-\beta H(0)}\hat{c}(t)\hat{c}^{\dagger}(t')]$, from which various thermodynamic observables can be calculated. In particular, the internal energy per lattice site (A.2) is given by

$$E(t) = \partial_t G^{<}(t, t')|_{t=t'}, \tag{A.2}$$

which follows directly from the equations of motion of the lattice system, assuming spatial homogeneity.

The DMFT equations for the Falicov–Kimball model with time-dependent interaction were stated in detail in [41] and the appendix of [75], where an analytical solution for the case of a sudden switch of the interaction parameter is given. The local Green function (A.1) is determined from the equations of motion [41],

$$G(t, t') = w_0 Q(t, t') + w_1 R(t, t'), \tag{A.3}$$

$$[\mathrm{i}\partial_t + \mu]Q(t, t') - [\Lambda * Q](t, t') = \delta_{\mathcal{C}}(t, t'), \tag{A.4}$$

$$[\mathrm{i}\partial_t + \mu - U(t)]R(t, t') - [\Lambda * R](t, t') = \delta_{\mathcal{C}}(t, t'), \tag{A.5}$$

where $w_1 = 1 - w_0$ denotes the average number of localized particles (which is fixed in the homogeneous phase), and $\Lambda(t, t')$ is the coupling to the environment, which is obtained by a self-consistency condition. The product $[A * B](t, t')$ denotes the convolution of two functions along the contour $\mathcal{C}$, and $\delta_{\mathcal{C}}(t, t')$ is the contour delta function. Throughout this paper we use the semi-elliptic density of states (6), in which case the self-consistency condition takes the simple form [41]

$$\Lambda(t, t') = V^2 G(t, t'). \tag{A.6}$$

Equations (A.3)–(A.6) form a closed set of integro-differential equation on $\mathcal{C}$. In this paper we consider also the case of a time-dependent hopping amplitude in (4), i.e. we assume $V_{ij}(t) \equiv V(t)t_{ij}$, where the hopping amplitude $V = V(0)$ sets the energy scale and the t_{ij} are dimensionless. This case can be mapped onto the case of a Hamiltonian with time-independent hopping and time-dependent interaction in the following way: the action $\exp[-\mathrm{i}\int \mathrm{d}t\, H(t)]$ of the lattice model is invariant under a simultaneous scaling of the Hamiltonian $\tilde{H}(t) = VH(t)/V(t)$ and transformation to new time variable $\tilde{t}(t) = \int_0^t \mathrm{d}t' V(t')/V$. By definition, $\tilde{H}$ has time-dependent interaction $\tilde{U}(t) = UV/V(t)$ but constant hopping V, such that equation (A.6) is valid. Under the same transformation of time variables, the hybridization function $\Lambda(t, t')$ transforms as $\tilde{\Lambda}(t_1, t_2) = V(t_1)\Lambda(t_1, t_2)V(t_2)/V^2$. Hence the change of the time variable leads to a replacement of the self-consistency equation (A.6) by

$$\Lambda(t, t') = V(t)G(t, t')V(t'). \tag{A.7}$$

By discretizing the contour $\mathcal{C}$, equations (A.3), (A.4), (A.5) and (A.7) can in principle be reduced to the inversion of a matrix whose dimension is given by the number of mesh points along $\mathcal{C}$ [64, 65]. This approach is not suitable here, because it would require an infinite length of the contour in the case of initial states at zero temperature ($\beta \to \infty$). A different approach first parametrizes contour Green functions in terms of various real and imaginary time components, and uses Langreth rules to derive separate integral equations for each component [74]. One can then remove the imaginary time branch by a partial Fourier transform to Matsubara frequencies and analytical continuation to real frequencies [70]. The solution of integro-differential equations such as (A.4) and (A.5) in this way is described in detail in [70]. In the following we will therefore only briefly restate these equations to mention the differences that arise from the fact that we are not solving a single equation (such as equation (A.4) for given Λ) but a nonlinear set of equations.

In the following we adopt the notation of [70]. When both time arguments of a contour Green function $A(t, t')$ are on the imaginary time portion of the contour, we obtain the Matsubara component, which can be represented in the form

$$A(-\mathrm{i}\tau, -\mathrm{i}\tau') = \frac{i}{\beta} \sum_n \mathrm{e}^{\mathrm{i}\omega_n(\tau'-\tau)} a(\mathrm{i}\omega_n). \tag{A.8}$$

The function $a(\omega)$ can be continued to real frequencies. Using this parametrization to rewrite equations (A.4) and (A.5) [70], we obtain the well-known cubic equations for the local Green function of the homogeneous phase in the Falicov–Kimball model [61]

$$g(\omega + \mathrm{i}0) = \frac{w_0}{\omega + \mu - V(0)^2 g(\omega + \mathrm{i}0)} + \frac{w_1}{\omega + \mu - U - V(0)^2 g(\omega + \mathrm{i}0)}. \tag{A.9}$$

The solution of this equation (with negative imaginary part) describes the initial state.

Next we consider the retarded component $A^{\mathrm{r}}(t, t') = \Theta(t - t')[A^{>}(t, t') - A^{<}(t, t')]$ of the contour Green function, for which equations (A.3), (A.4), (A.5) and (A.7) read [47]

$$G^{\mathrm{r}}(t, t') = w_0 Q^{\mathrm{r}}(t, t') + w_1 R^{\mathrm{r}}(t, t'), \tag{A.10}$$

$$[\mathrm{i}\partial_t + \mu] Q^{\mathrm{r}}(t, t') - \int_{t'}^{t} \mathrm{d}s\, V(t) G^{\mathrm{r}}(t, s) V(s) Q^{\mathrm{r}}(s, t') = 0, \tag{A.11}$$

$$[\mathrm{i}\partial_t + \mu - U] R^{\mathrm{r}}(t, t') - \int_{t'}^{t} \mathrm{d}s\, V(t) G^{\mathrm{r}}(t, s) V(s) R^{\mathrm{r}}(s, t') = 0. \tag{A.12}$$

These equations must be solved for $t > t'$ with the initial condition $G^{\mathrm{r}}(t, t) = R^{\mathrm{r}}(t, t) = Q^{\mathrm{r}}(t, t) = -i$. In contrast to the case discussed in [70], this is a set of *nonlinear* integro-differential equations. However, the equations are causal in the sense that the differential is always determined by an integral over the function at *earlier* times. Hence the solution of equations (A.10)–(A.11) is very similar to the solution of an ordinary differential equation, and the presence of a nonlinearity does not lead to additional difficulties.

In addition to equations for the retarded and Matsubara components, one has to consider equations for the mixed components $A^{\ulcorner}(t, \tau) \equiv A(t, -\mathrm{i}\tau)$. In terms of the partial Fourier transform

$$A^{\ulcorner}(t, \mathrm{i}\omega_n) = \int_0^{\beta} \mathrm{d}\tau\, A^{\ulcorner}(t, \tau) \mathrm{e}^{-\mathrm{i}\omega_n \tau}, \tag{A.13}$$

we obtain, after analytically continuing $i\omega_n \to \omega_\pm \equiv \omega \pm i0$,

$$G^\neg(t,\omega_\pm) = w_0 Q^\neg(t,\omega_\pm) + w_1 R^\neg(t,\omega_\pm), \tag{A.14}$$

$$[i\partial_t + \mu]Q^\neg(t,\omega_\pm) - \int_0^t ds\, V(t)G^{\mathrm{r}}(t,s)V(s)Q^\neg(s,\omega_\pm) = V(t)G^\neg(t,\omega_\pm)V(0)q^{\mathrm{M}}(\omega_\pm), \tag{A.15}$$

$$[i\partial_t + \mu - U]R^\neg(t,\omega_\pm) - \int_0^t ds\, V(t)G^{\mathrm{r}}(t,s)V(s)R^\neg(s,\omega_\pm) = V(t)G^\neg(t,\omega_\pm)V(0)r^{\mathrm{M}}(\omega_\pm), \tag{A.16}$$

to be solved with the initial condition $A^\neg(0,\omega_\pm) = ia^{\mathrm{M}}(\omega_\pm)$. Finally, the lesser component satisfies

$$G^<(t,t') = w_0 Q^<(t,t') + w_1 R^<(t,t'), \tag{A.17}$$

$$\begin{aligned}
&[i\partial_t + \mu]Q^<(t,t') - \int_0^t ds\, V(t)G^{\mathrm{r}}(t,s)V(s)Q^<(s,t') \\
&= -V(t)V(0)\int \frac{d\omega}{2\pi} f(\omega)\left[G^\neg(t,\omega^+)Q^\neg(\omega^+,t') - G^\neg(t,\omega^-)Q^\neg(\omega^-,t')\right] \\
&\quad + \int_0^{t'} ds\, V(t)G^<(t,s)V(s)Q^{\mathrm{a}}(s,t'),
\end{aligned} \tag{A.18}$$

$$\begin{aligned}
&[i\partial_t + \mu - U]R^<(t,t') - \int_0^t ds\, V(t)G^{\mathrm{r}}(t,s)V(s)R^<(s,t') \\
&= -V(t)V(0)\int \frac{d\omega}{2\pi} f(\omega)\left[G^\neg(t,\omega^+)R^\neg(\omega^+,t') - G^\neg(t,\omega^-)R^\neg(\omega^-,t')\right] \\
&\quad + \int_0^{t'} ds\, V(t)G^<(t,s)V(s)R^{\mathrm{a}}(s,t'),
\end{aligned} \tag{A.19}$$

to be solved with the initial condition $A^<(0,t) = A^\neg(0,t)$ for $A = Q, R$. Together with the Hermitian symmetry, $A^{\mathrm{a}}(t,t') = A^{\mathrm{r}}(t',t)^*$ and $A^\neg(t,\omega) = A^\neg(\omega^*,t)^*$ for Q, R and G, the set of equations is closed.

Note that the expansion of equations (A.3), (A.4), (A.5) and (A.7) into equations (A.10)–(A.19) has the following technical advantage. The numerical solution of Volterra integro-differential equations can be easily implemented such that the time discretization error scales as $\epsilon \sim \Delta t^p = (\tau/N)^p$ for $\Delta t \to 0$, with $p > 1$ [76]. To study the excitation energy (3) for large τ from the difference (2), the absolute energy (A.2) must be determined with a relative accuracy of the order of $\tau^{-\eta}$. Assuming the above error scaling, sufficient accuracy of the energy with respect to $\Delta E(\tau)$ thus requires $N \sim \tau^{1+\eta/p}$ time steps for $\tau \to \infty$. On the other hand, the Green function must be stored at $\mathcal{O}(N^2)$ time points and hence N is the limiting numerical factor (we go up to $N \approx 10\,000$). It is thus crucial to use an algorithm that is correct up to high order in Δt when the exponent η is large. For ramps in the insulating phase, e.g. $\eta \geqslant 2$ is found (cf equation (9)), and these results could not be obtained using the lowest-order trapezoid approximation ($p = 1$), but we used higher-order schemes instead ($p = 5$).

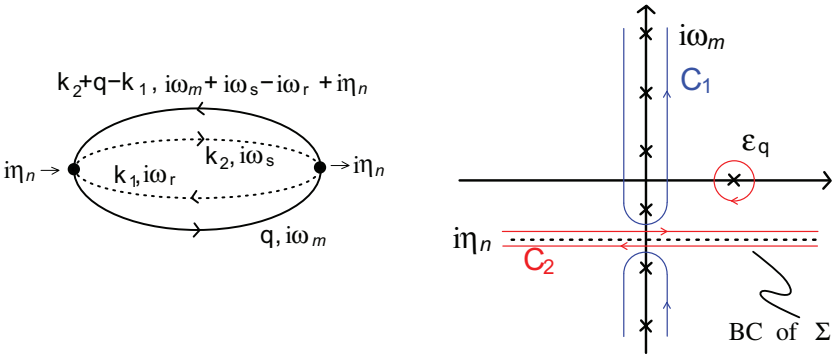

Figure A.1. Left panel: diagrammatic representation of equation (B.3). Lines represent the noninteracting momentum-resolved Green function $g^0_{q\sigma}(\mathrm{i}\omega_m) = 1/(\mathrm{i}\omega_m - \epsilon_{q\sigma})$ for $\sigma = \uparrow$ (solid lines) and $\sigma = \downarrow$ (dashed lines). Momentum is conserved at the vertices, frequency $\mathrm{i}\eta_n$ enters at the left vertex. Right panel: transformation of the Matsubara sum (B.5) to the real frequency interval (B.6), using the usual expression $\sum_{\mathrm{i}\omega_m} w(\mathrm{i}\omega_m) = (\mathrm{i}\beta/2\pi)\oint_{C_1} \mathrm{d}z f(z) w(z)$, where $f(z)$ is the Fermi function and $w(z)$ is some analytic integrand. The integrand in equation (B.5) has a branch cut at $z = -\mathrm{i}\eta_n$ due to the branch cut of $\Sigma(z)$ along the real axis, and a pole at $\epsilon_{q\uparrow}$. Then the contour C_1 is transformed into C_2, which yields (B.5), using the fact that the Fermi function is periodic under shift with bosonic Matsubara frequencies, $f(\omega - \mathrm{i}\eta_n) = f(\omega)$.

Appendix B. Excitation density in the noninteracting limit of the Hubbard and the Falicov–Kimball models

For a ramp of the interaction strength in the Hubbard model and the Falicov–Kimball model, the operator in equation (10) is given by the double occupation (32), and the excitation density $R(\omega)$ can be evaluated at $U = 0$. For this purpose we introduce the imaginary-time-ordered correlation function

$$\tilde{R}(\tau - \tau') = \langle T_\tau D(\tau) D(\tau')] \rangle_0 \tag{B.1}$$

where the expectation value $\langle \cdot \rangle = \mathrm{Tr}[\mathrm{e}^{-\beta H} \cdot]/\mathrm{Tr}[\mathrm{e}^{-\beta H_0}]$ is taken in the noninteracting state at temperature $T = 1/\beta$ (the limit $T \to 0$ is taken at the end), and D is given by (32). (T_τ is the imaginary time ordering operator, and $D(\tau)$ are Heisenberg operators with respect to H_0.) Because D contains an even number of Fermi operators, the function $\tilde{R}(\tau)$ satisfies periodic boundary conditions on the imaginary time contour $\tau \in [0, \beta]$ and can be expanded in bosonic Matsubara frequencies $\eta_n = 2\pi n/T$, $\tilde{R}(\mathrm{i}\eta_n) = \int_0^\beta \mathrm{d}\tau \tilde{R}(\tau) \mathrm{e}^{-\mathrm{i}\eta_n \tau}$. Using the Lehmann representation one can show that the excitation density (18) may be obtained from the unique analytical continuation of $\tilde{R}(\mathrm{i}\eta_n)$ from $\eta_n > 0$ to the upper half of the complex frequency plane,

$$R(\omega) = -\frac{1}{\pi} \mathrm{Im}\, \tilde{R}(\omega + \mathrm{i}0). \tag{B.2}$$

To calculate $\tilde{R}$, the expectation value (B.1) is factorized using Wick's theorem and transformed to bosonic Matsubara frequencies. It turns out that the only nonvanishing

contractions for $\eta_n \neq 0$ are given by

$$\tilde{R}(i\eta_n) \overset{n\neq 0}{=} \sum_{\boldsymbol{k}_1,\boldsymbol{k}_2,\boldsymbol{q}} \sum_{r,s,m} g^0_{\boldsymbol{q}\downarrow}(\mathrm{i}\omega_m) g^0_{\boldsymbol{k}_2\uparrow}(\mathrm{i}\omega_s) g^0_{\boldsymbol{k}_1\uparrow}(\mathrm{i}\omega_r) g^0_{\boldsymbol{k}_2-\boldsymbol{q}-\boldsymbol{k}_1,\downarrow}(\mathrm{i}\omega_m + \mathrm{i}\omega_s - \mathrm{i}\omega_r + \mathrm{i}\eta_n), \tag{B.3}$$

where $g^0_{\boldsymbol{q}\sigma}(\mathrm{i}\omega_m) = 1/(\mathrm{i}\omega_m - \epsilon_{\boldsymbol{q}\sigma})$ is the noninteracting Green function at momentum $\boldsymbol{q}$, and $\mathrm{i}\omega_m$ are fermionic Matsubara frequencies. The expression has a simple diagrammatic representation (figure A.1 (left panel). The diagram is split into one Green function line $g^0_{\boldsymbol{q}\downarrow}(\mathrm{i}\omega_m)$ and the remainder, which we identify as the second-order contribution $\Sigma^{(2)}_{\boldsymbol{q}\downarrow}$ to the self-energy,

$$\tilde{R}(\mathrm{i}\eta_n) = \sum_{\boldsymbol{q}} \sum_{i\omega_m} g^0_{\boldsymbol{q}\downarrow}(\mathrm{i}\omega_m) \Sigma^{(2)}_{\boldsymbol{q}\downarrow}(\mathrm{i}\eta_n + \mathrm{i}\omega_m). \tag{B.4}$$

One can now transform the Matsubara summation into a frequency integral, where it must be taken into account that the self-energy $\Sigma(z)$ has a branch cut along the real axis with $\Sigma(\omega \pm \mathrm{i}0) \equiv \mp \mathrm{Im}\,\Sigma(\omega)$ (figure A.1 (right panel). The result is

$$\tilde{R}(\mathrm{i}\eta_n) = \sum_{\boldsymbol{q}} \left[f(\epsilon_{\boldsymbol{q}\uparrow}) \Sigma^{(2)}_{\boldsymbol{q}\uparrow}(\mathrm{i}\eta_n + \epsilon_{\boldsymbol{q}\uparrow}) - \frac{1}{\pi} \int \mathrm{d}\omega\, f(\omega) \frac{\mathrm{Im}\,\Sigma^{(2)}_{\boldsymbol{q}\uparrow}(\omega + \mathrm{i}0)}{\omega - \mathrm{i}\eta_n - \epsilon_{\boldsymbol{q}\uparrow}} \right], \tag{B.5}$$

where $f(\epsilon)$ is the Fermi function. Equation (B.5) is finally continued to the real frequencies by replacing $\mathrm{i}\eta_n \to \omega + \mathrm{i}0$, and the spectrum (B.2) is obtained as

$$R(\omega) = \frac{1}{\pi} \sum_{\boldsymbol{q}} [f(\omega + \epsilon_{\boldsymbol{q}\downarrow}) - f(\epsilon_{\boldsymbol{q}\downarrow})] \mathrm{Im}\,\Sigma^{(2)}_{\boldsymbol{q}\downarrow}(\omega + \epsilon_{\boldsymbol{q}\downarrow}). \tag{B.6}$$

Then, taking the limit of zero initial temperature yields equation (33).

References

[1] Born M and Fock V A 1928 *Z. Phys.* A **51** 165
[2] Kato T 1950 *J. Phys. Soc. Japan* **5** 435
[3] Avron J E and Elgart A 1999 *Commun. Math. Phys.* **203** 445
[4] Landau L D 1932 *Phys. Z. Sowjetunion* **2** 46
[5] Zener C 1932 *Proc. R. Soc.* A **137** 696
[6] Brundobler S and Elser V 1993 *J. Phys. A: Math. Gen.* **26** 1211
[7] Shytov A V 2004 *Phys. Rev.* A **70** 052708
[8] Volkov M V and Ostrovsky V N 2004 *J. Phys. B: At. Mol. Opt. Phys.* **37** 4069
[9] Dobrescu B E and Sinitsyn N A 2006 *J. Phys. B: At. Mol. Opt. Phys.* **39** 1253
[10] Ostrovsky V N and Volkov M V 2006 *Phys. Rev.* B **73** 060405
[11] Bloch I, Dalibard J and Zwerger W 2008 *Rev. Mod. Phys.* **80** 885
[12] Zenesini A, Lignier H, Tayebirad G, Radogostowicz J, Ciampini D, Mannella R, Wimberger S, Morsch O and Arimondo E 2009 *Phys. Rev. Lett.* **103** 090403
[13] Barouch E, McCoy B M and Dresden M 1970 *Phys. Rev.* A **2** 1075
[14] Polkovnikov A 2005 *Phys. Rev.* B **72** 161201
[15] Zurek W H, Dorner U and Zoller P 2005 *Phys. Rev. Lett.* **95** 105701
[16] Dziarmaga J 2005 *Phys. Rev. Lett.* **95** 245701
[17] Barankov R and Levitov L S 2006 *Phys. Rev.* A **73** 033614
[18] Damski B and Zurek W H 2006 *Phys. Rev.* A **73** 063405
[19] Wubs M, Saito K, Kohler S, Hänggi P and Kayanuma Y 2006 *Phys. Rev. Lett.* **97** 200404
[20] Dziarmaga J 2006 *Phys. Rev.* B **74** 064416

[21] Cucchietti F M, Damski B, Dziarmaga J and Zurek W H 2007 *Phys. Rev.* A **75** 023603
[22] Klich I, Lannert C and Refael G 2007 *Phys. Rev. Lett.* **99** 205303
[23] Altland A and Gurarie V 2008 *Phys. Rev. Lett.* **100** 063602
[24] Polkovnikov A and Gritsev V 2008 *Nat. Phys.* **4** 477
[25] Barankov R and Polkovnikov A 2008 *Phys. Rev. Lett.* **101** 076801
[26] Sen D, Sengupta K and Mondal S 2008 *Phys. Rev. Lett.* **101** 016806
[27] Tomadin A, Mannella R and Wimberger S 2008 *Phys. Rev.* A **77** 013606
[28] Itin A P and Törmä P 2009 arXiv:0901.4778
[29] De Grandi C and Polkovnikov A 2009 arXiv:0910.2236 (Published in *Quantum Quenching, Annealing and Computation* (*Lecture Notes in Physics* vol 802) (Berlin: Springer))
[30] De Grandi C, Gritsev V and Polkovnikov A 2009 arXiv:0910.0876
[31] Divakaran U, Dutta A and Sen D 2010 *Phys. Rev.* B **81** 054306
[32] Moeckel M and Kehrein S 2010 *New J. Phys.* **12** 055016
[33] De Grandi C, Gritsev V and Polkovnikov A 2010 *Phys. Rev.* B **81** 012303
[34] Heims S P 1965 *Am. J. Phys.* **33** 722
[35] Girardeau M D 1969 *Phys. Lett.* A **30** 442
[36] Sengupta K, Powell S and Sachdev S 2004 *Phys. Rev.* A **69** 053616
[37] Cazalilla M A 2006 *Phys. Rev. Lett.* **97** 156403
[38] Rigol M, Dunjko V, Yurovsky V and Olshanii M 2007 *Phys. Rev. Lett.* **98** 050405
[39] Kollath C, Läuchli A and Altman E 2007 *Phys. Rev. Lett.* **98** 180601
[40] Manmana S R, Wessel S, Noack R M and Muramatsu A 2007 *Phys. Rev. Lett.* **98** 210405
[41] Eckstein M and Kollar M 2008 *Phys. Rev. Lett.* **100** 120404
[42] Möckel M and Kehrein S 2008 *Phys. Rev. Lett.* **100** 175702
[43] Kollar M and Eckstein M 2008 *Phys. Rev.* A **78** 013626
[44] Rigol M, Dunjko V and Olshanii M 2008 *Nature* **452** 854
[45] Rossini D, Silva A, Mussardo G and Santoro G E 2009 *Phys. Rev. Lett.* **102** 127204
[46] Barmettler P, Punk M, Gritsev V, Demler E and Altman E 2009 *Phys. Rev. Lett.* **102** 130603
[47] Eckstein M, Kollar M and Werner P 2009 *Phys. Rev. Lett.* **103** 056403
[48] Kinoshita T, Wenger T and Weiss D S 2006 *Nature* **440** 900
[49] Vitanov N V 1999 *Phys. Rev.* A **59** 988
[50] Reischl A, Schmidt K P and Uhrig G S 2005 *Phys. Rev.* A **72** 063609
[51] Rey A M, Pupillo G and Porto J V 2006 *Phys. Rev.* A **73** 023608
[52] Ho T-L and Zhou Q 2007 *Phys. Rev. Lett.* **99** 120404
[53] Yoshimura S, Konabe S and Nikuni T 2008 *Phys. Rev.* A **78** 015602
[54] Cramer M, Ospelkaus S, Ospelkaus C, Bongs K, Sengstock K and Eisert J 2008 *Phys. Rev. Lett.* **100** 140409
[55] Pollet L, Kollath C, Van K Houcke and Troyer M 2008 *New J. Phys.* **10** 065001
[56] Falicov L M and Kimball J C 1969 *Phys. Rev. Lett.* **22** 997
[57] Georges A, Kotliar G, Krauth W and Rozenberg M J 1996 *Rev. Mod. Phys.* **68** 13
[58] Metzner W and Vollhardt D 1989 *Phys. Rev. Lett.* **62** 324
[59] Brandt U and Mielsch C 1989 *Z. Phys. B: Condens. Matter* **75** 365
[60] van Dongen P G J and Vollhardt D 1990 *Phys. Rev. Lett.* **65** 1663
[61] van Dongen P G J 1992 *Phys. Rev.* B **45** 2267
[62] Freericks J K and Zlatić V 2003 *Rev. Mod. Phys.* **75** 1333
[63] Schmidt P and Monien H 2002 arXiv:cond-mat/0202046 unpublished
[64] Freericks J K, Turkowski V M and Zlatić V 2006 *Phys. Rev. Lett.* **97** 266408
[65] Freericks J K 2008 *Phys. Rev.* B **77** 075109
[66] Tran M-T 2008 *Phys. Rev.* B **78** 125103
[67] Joura A V, Freericks J K and Pruschke T 2008 *Phys. Rev. Lett.* **101** 196401
[68] Tsuji N, Oka T and Aoki H 2008 *Phys. Rev.* B **78** 235124

[69] Tsuji N, Oka T and Aoki H 2009 *Phys. Rev. Lett.* **103** 047403
[70] Eckstein M, Kollar M and Werner P 2010 *Phys. Rev.* B **81** 115131
[71] Olver F W J 1997 *Asymptotics and Special Functions* (Wellesley, MA: AK Peters)
[72] Rigolin G, Ortiz G and Ponce V H 2008 *Phys. Rev.* A **78** 052508
[73] Müller-Hartmann E 1989 *Z. Phys.* B **76** 211
[74] van Leeuwen R, Dahlen N E, Stefanucci G, Almbladh C-O and von Barth U 2005 arXiv:cond-mat/0506130v1 (Published in Marques MAL, Ullrich CA, Nogueira F, Rubio A, Burke K and Gross EKU (ed) 2006 *Time-Dependent Density Functional Theory* (*Lecture Notes in Physics* vol 706) (Berlin: Springer))
[75] Eckstein M and Kollar M 2008 *Phys. Rev.* B **78** 245113
[76] Brunner H and van der Houwen P J 1986 *The Numerical Solution of Volterra Equations* (Amsterdam: North-Holland)